LETTERS

Sarcolemma-localized nNOS is required to maintain activity after mild exercise

Yvonne M. Kobayashi[1,2,3,4], Erik P. Rader[1,2,3,4], Robert W. Crawford[1,2,3,4], Nikhil K. Iyengar[4], Daniel R. Thedens[5], John A. Faulkner[7], Swapnesh V. Parikh[4], Robert M. Weiss[4], Jeffrey S. Chamberlain[8], Steven A. Moore[6] & Kevin P. Campbell[1,2,3,4]

Many neuromuscular conditions are characterized by an exaggerated exercise-induced fatigue response that is disproportionate to activity level. This fatigue is not necessarily correlated with greater central or peripheral fatigue in patients[1], and some patients experience severe fatigue without any demonstrable somatic disease[2]. Except in myopathies that are due to specific metabolic defects, the mechanism underlying this type of fatigue remains unknown[2]. With no treatment available, this form of inactivity is a major determinant of disability[3]. Here we show, using mouse models, that this exaggerated fatigue response is distinct from a loss in specific force production by muscle, and that sarcolemma-localized signalling by neuronal nitric oxide synthase (nNOS) in skeletal muscle is required to maintain activity after mild exercise. We show that *nNOS*-null mice do not have muscle pathology and have no loss of muscle-specific force after exercise but do display this exaggerated fatigue response to mild exercise. In mouse models of nNOS mislocalization from the sarcolemma, prolonged inactivity was only relieved by pharmacologically enhancing the cGMP signal that results from muscle nNOS activation during the nitric oxide signalling response to mild exercise. Our findings suggest that the mechanism underlying the exaggerated fatigue response to mild exercise is a lack of contraction-induced signalling from sarcolemma-localized nNOS, which decreases cGMP-mediated vasomodulation in the vessels that supply active muscle after mild exercise. Sarcolemmal nNOS staining was decreased in patient biopsies from a large number of distinct myopathies, suggesting a common mechanism of fatigue. Our results suggest that patients with an exaggerated fatigue response to mild exercise would show clinical improvement in response to treatment strategies aimed at improving exercise-induced signalling.

To understand the molecular basis of the exercise-induced fatigue response, we studied genetically defined mouse models. We designed an integrative *in vivo* assay to test conscious mice, subjecting the mice to brief low-speed treadmill exercise followed by testing in an open-field activity chamber (see Methods). We first assessed two dystrophic mouse lines, *mdx* (model for Duchenne muscular dystrophy)[4] and *Sgca*-null (model for limb-girdle muscular dystrophy type 2D that is deficient for the gene encoding α-sarcoglycan (*Sgca*))[5]. In the absence of previous exercise, activity in these mice was indistinguishable from that of wild-type mice (Fig. 1a, b, and Supplementary Videos 1a–d). After a single trial of mild exercise, significant differences were observed (Fig. 1a, b, and Supplementary Videos 2a–d): the *mdx* and *Sgca*-null mice showed a significant decrease in vertical activity.

The decrease in vertical activity among *mdx* and *Sgca*-null mice did not correlate with differences in extensor digitorum longus (EDL)-specific force measurements relative to those taken in C57BL/6 mice before exercise (Fig. 1c). Moreover, *Sgca*-null mice do not develop brain, heart or vascular pathology[6], and they have muscle-force values similar to those of control mice[7]. Therefore, neither cardiac deficiency nor an inability to produce force was the cause of the post-exercise inactivity in the *Sgca*-null mice. Because inflammation is a feature of dystrophinopathy[4], chronic fatigue is associated with muscle pain, and chronic pain is associated with fatigue[8], we treated *mdx* mice with either deflazacort or ibuprofen. However, neither treatment resulted in improved post-exercise activity (Fig. 1d), suggesting that the inactivity occurring immediately after mild exercise in *mdx* mice was not due to inflammation or pain. Overall, the results of our exercise–activity assay implied that the exaggerated fatigue response in these mice was not attributable to cardiac deficiency, inflammation, pain or lack of muscle force.

To test whether the exercise-induced inactivity in the *mdx* and *Sgca*-null mice was due to the genetically determined structural defect in muscle, we assayed two mouse models in which the muscle pathology related to the specific dystrophin glycoprotein complex (DGC) defect is rescued—microdystrophin/*mdx* and MCKεSG/*Sgca*-null. In microdystrophin/*mdx* mice (a model for mild Becker muscular dystrophy[9]—the DGC has a mutated but functional dystrophin), microdystrophin is expressed in *mdx* mouse muscle. In the MCKεSG/*Sgca*-null mice, ε-sarcoglycan is expressed in mouse muscle that is deficient for *Sgca* (Supplementary Fig. 1). Neither rescue strain showed pathological signs of muscular dystrophy, and the skeletal muscle DGC of both was recovered at the biochemical, structural and functional levels (refs 9, 10 and Supplementary Figs 1 and 2).

Despite having a structurally intact skeletal muscle DGC, microdystrophin/*mdx* mice experience a substantial decrease in activity after mild exercise, like their *mdx* littermates (Fig. 1e). Because patients with Becker muscular dystrophy show profound fatigue after light exertion[11], and loss of sarcolemma-localized nNOS serves as a diagnostic indicator of some forms of Becker muscular dystrophy[12], a possible reason for the post-exercise inactivity is a loss of sarcolemma-localized nNOS. To test this possibility we probed for nNOS localization in microdystrophin/*mdx* skeletal muscle and found that the DGC generated in this rescue strain failed to recruit nNOS to the sarcolemma (Fig. 1e, inset). These data are in agreement with recent reports on microdystrophin expression in dystrophin-deficient mouse models[13]. Moreover, the data suggest that exercise-

[1]Howard Hughes Medical Institute, [2]Department of Molecular Physiology and Biophysics, [3]Department of Neurology, [4]Department of Internal Medicine, [5]Department of Radiology, [6]Department of Pathology, University of Iowa, Roy J. and Lucille A. Carver College of Medicine, 4283 Carver Biomedical Research Building, 285 Newton Road, Iowa City, Iowa 52242-1101, USA. [7]Department of Molecular and Integrative Physiology, University of Michigan, 2031 Biomedical Sciences Research Building, Ann Arbor, Michigan 48109-2200, USA. [8]Department of Neurology, University of Washington School of Medicine, HSB, Room K243b, Seattle, Washington 98195-7720, USA.

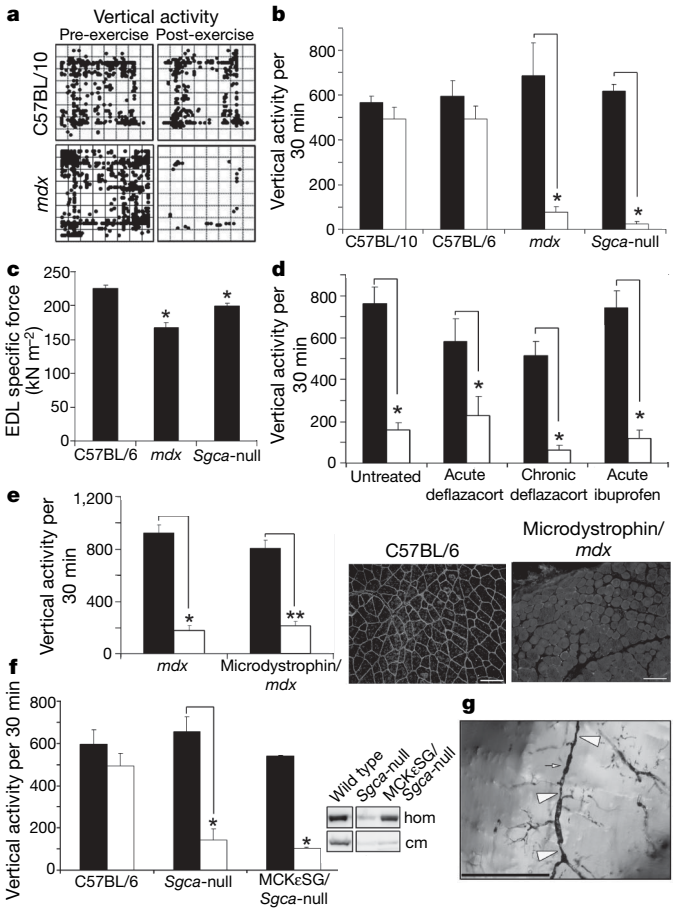

Figure 1 | Loss of sarcolemma-localized nNOS leads to skeletal muscle vascular narrowings, decreased capillary perfusion and an exaggerated fatigue response after mild exercise in dystrophic and non-dystrophic mouse models. **a**, Representative vertical activity tracings of zone maps for C57BL/10 and *mdx* mice before and after exercise. **b**, Quantified vertical activity before (filled columns) and after (open columns) exercise for C57BL/10, C57BL/6, *mdx* and *Sgca*-null mouse strains ($n = 6$ for each strain). Asterisk, $P = 0.012$. **c**, EDL muscle-specific force measurements from C57BL/6 ($n = 6$), *mdx* ($n = 4$) and *Sgca*-null ($n = 4$) mice. Asterisk, $P < 0.05$. **d**, Pre-exercise (filled columns) and post-exercise (open columns) vertical activity in untreated ($n = 7$) and anti-inflammatory treated *mdx* mice, acutely ($n = 4$) or chronically ($n = 4$) with deflazacort or acutely with ibuprofen ($n = 5$). Asterisk, $P < 0.003$. **e**, Left panel: quantified pre-exercise (filled columns) and post-exercise (open columns) vertical activity for microdystrophin/*mdx* mice ($n = 6$) and their *mdx* littermates ($n = 4$). Asterisk, $P = 0.005$; two asterisks, $P < 0.0001$. The right panels show representative immunofluorescence images of nNOS detection in the gastrocnemius muscles from C57BL/6 and microdystrophin/*mdx* mice. **f**, Quantified pre-exercise (filled columns) and post-exercise (open columns) vertical activity for MCKεSG/*Sgca*-null mice ($n = 6$) and their *Sgca*-null littermates ($n = 6$). Asterisk, $P < 0.0001$. Inset: immunoblot detection of total nNOS from homogenates (hom), and crude skeletal muscle membranes (cm). **g**, Representative Microfil image of skeletal muscle vessels of MCKεSG/*Sgca*-null mice after exercise—large arrowheads mark extended areas of vascular narrowing; the small arrow marks a shorter stretch of radial vascular narrowing. Error bars indicate s.e.m.

induced inactivity in the microdystrophin/*mdx* mice is not caused directly by a structurally defective muscle DGC, and that loss of sarcolemmal nNOS does not negatively affect muscle contractility. Thus, sarcolemmal nNOS seems to act at the level of post-exercise activity.

In contrast to the microdystrophin/*mdx* mice, MCKεSG/*Sgca*-null mice have structurally intact DGC in the brain and the vasculature, but express ε-sarcoglycan instead of α-sarcoglycan in the DGC of muscle. Our exercise–activity assay showed that post-exercise activity in the MCKεSG/*Sgca*-null mice was substantially decreased relative to that in C57BL/6 mice but similar to that in *Sgca*-null and *mdx* mice (Fig. 1b, f). Because the microdystrophin-containing DGC failed to recruit nNOS, we speculated that the MCKεSG/*Sgca*-null mice would also fail to localize nNOS to the sarcolemma. Indeed, although total nNOS levels in muscle homogenates from MCKεSG/*Sgca*-null mice were similar to those in the wild type, nNOS from the rescue model failed to purify together with the ε-sarcoglycan-containing DGC in the membrane preparation (Fig. 1f, inset). Taken together, these results are compatible with the notion that the exaggerated fatigue response is not directly related to a structurally defective muscle DGC or to muscle weakness, but rather to a failure in the sarcolemmal localization of nNOS.

Because sarcolemma-localized nNOS is crucial for maintaining vasomodulation to contracting muscles[14], we tested whether communication from skeletal muscle to the local blood supply is deficient after mild exercise by perfusing MCKεSG/*Sgca*-null mouse arteries before or after exercise with Microfil and examined the skeletal muscle vasculature (Fig. 1g). We identified vascular narrowings of various lengths along the arteries that feed the skeletal muscles in the post-exercise samples only, and also noted the lack of perfusion of capillaries. The *mdx* and microdystrophin/*mdx* mice similarly showed skeletal muscle vascular narrowings only after exercise and also a lack of perfusion of capillaries (Supplementary Fig. 3c and data not shown). This phenotype is consistent with inefficient contraction-induced muscle nNOS signalling to local blood vessels. Overall, these data imply that loss of sarcolemma-localized nNOS causes deficient exercise-induced vasomodulation in skeletal muscle, and that these lead to prolonged inactivity after mild exercise.

To directly examine the contribution of NO generated by endothelial NOS (eNOS) or nNOS to the exaggerated fatigue response, we tested both *nNOS*-null and *eNOS*-null mice in our exercise–activity assay. Mice deficient for nNOS express normal levels of the DGC components at the sarcolemma and have histologically normal muscle[15–17]. Reports suggest that both mouse strains have defective vasoregulation[18,19]; however, *mdx* and *nNOS*-null mice have a normal α-adrenergic vasoconstrictive response to exercise[20]. Vertical pre-exercise activities were similar in *eNOS*-null, *nNOS*-null and C57BL/6 mice, suggesting that the loss of either NOS does not affect mouse activity (Fig. 2a). After exercise, however, *nNOS*-null vertical activity decreased significantly (Fig. 2a). Serum creatine kinase levels before and after exercise for each of the *NOS*-null mice were similar to those in C57BL/6 mice and low compared with *mdx* mice (Fig. 2b), and there were no signs of muscle pathology in sections from *nNOS*-null quadriceps muscle (Supplementary Fig. 4b), suggesting that muscle damage and necrosis were not the causes of the post-exercise inactivity. We then tested whether post-exercise muscle contractility affected the ability of C57BL/6 and *nNOS*-null skeletal muscle to produce force after mild exercise. We found that the specific force of EDL muscles after exercise was not significantly affected in *nNOS*-null muscle in comparison with C57BL/6 muscle (Supplementary Fig. 4c). Because lack of muscle contractility was not causing the inactivity in the *nNOS*-null mice after exercise, we checked whether *NOS*-null mice had post-exercise skeletal muscle vascular narrowings and lack of capillary perfusion similar to those in the dystrophic and rescue mice. Microfil perfusion of arteries from *NOS*-null mice before and after exercise revealed the lack of capillary perfusion and also the presence of vascular narrowings only in post-exercise *nNOS*-null skeletal muscle (Fig. 2c). We also found that treating wild-type mice with either the nNOS-specific inhibitor 3-bromo-7-nitroindazole or the vasoconstrictor sarafotoxin 6c caused post-exercise inactivity (Fig. 2d). These findings suggest that a deficiency of sarcolemma-localized nNOS causes exercise-induced narrowing of the vasculature that feeds active muscles after exercise, thereby promoting prolonged inactivity after mild exercise.

To test whether the vascular effect on post-exercise activity was from NO or was downstream of the NO signal, we bypassed

sarcolemmal nNOS signalling for decreasing vasoconstriction by treating *mdx* mice with a panel of pharmacological agents that promote vasodilation; we found that the exaggerated fatigue response was alleviated only by treatment with a phosphodiesterase (PDE) 5A inhibitor (Supplementary Fig. 6), suggesting that the fatigue that we saw depended on cGMP, which acts downstream of NO production. PDE activity in *mdx* mice is 2–6-fold higher than in C57BL/10 mice[21], which is consistent with the elevated PDE activity in human muscular disorders[18,21,22]. We treated *nNOS*-null, MCKεSG/*Sgca*-null and *mdx* mice with PDE5A inhibitors and tested them in our exercise–activity assay; we found that the treated MCKεSG/*Sgca*-null and *mdx* mice showed an increase in post-exercise activity (Fig. 2e and Supplementary Fig. 7a–d). Because inhibition of PDE5A had no effect on activity before exercise, our results suggest that PDE5A inhibition is alleviating the exaggerated fatigue response by enhancing the cGMP signal produced by contraction-induced nNOS stimulation. Although downstream effectors of cGMP are numerous and divergent[23], the half-life of cGMP can be affected by the activity of PDE5A. Our data indicate that the elevated PDE activity in extracts from *mdx* mice could be PDE5A activity, and that PDE activity could also be elevated in the rescue mouse models we tested.

Our data suggest that the local resistance of arterioles that perfuse sarcolemmal nNOS-deficient muscles increases during exercise and that the lack of activity after mild exercise will lead to muscle oedema. We examined blood flow before and after exercise with laser Doppler imaging and found that blood flow in *mdx* mice failed to increase as it did in C57BL/6 mice (Fig. 3a and Supplementary Fig. 7a), but treatment of *mdx* mice with a PDE5A inhibitor alleviated this defect (Fig. 3b) and increased muscle capillary perfusion (Fig. 3c). Given that insufficient relief of local vasoconstriction in active muscles can lead to muscle oedema[24], and that boys with Duchenne muscular dystrophy show muscle oedema[25], we looked for changes in water compartmentalization and dynamics in the hindleg muscles of *nNOS*-null, C57BL/10 and *mdx* mice before and after exercise by using spin–spin relaxation time (T_2)-magnetic resonance imaging. The *nNOS*-null mice did not have muscle damage or loss of contractility after exercise (Fig. 2b and Supplementary Fig. 4b, c), nor did they have muscle oedema (Supplementary Fig. 8a), suggesting that their lack of muscle damage prevents water accumulation in the tissue. Similarly, C57BL/10 mice showed little to no oedema in hindleg muscles after exercise (0.70 ± 0.50% (mean ± s.e.m.)) (Fig. 3f and

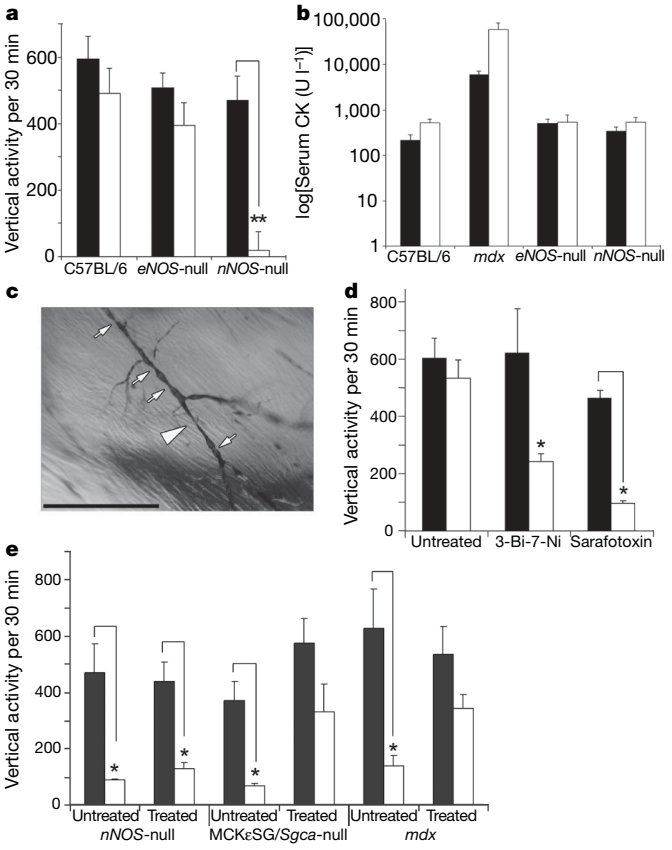

Figure 2 | Enhancing the cGMP signal resulting from muscle nNOS activation decreases the exaggerated fatigue response to mild exercise. **a**, Comparison of vertical activity before (filled columns) and after (open columns) exercise between C57BL/6, *eNOS*-null and *nNOS*-null mice ($n = 6$ for each). Two asterisks, $P < 0.001$. **b**, Serum creatine kinase (CK) levels before (filled columns) and after (open columns) exercise in C57BL/6 ($n = 6$), *eNOS*-null ($n = 4$) and *nNOS*-null ($n = 6$) mice, compared with *mdx* mice ($n = 6$). **c**, Representative Microfil image of *nNOS*-null quadriceps skeletal muscle arteries after exercise—the large arrowhead marks the extended area of vascular narrowing; small arrows mark shorter areas of radial vascular narrowing. Scale bar, 100 μm. **d**, Pre-exercise (filled columns) and post-exercise (open columns) vertical activities in untreated wild-type (C57BL/6 and C57BL/10) mice ($n = 4$), compared with 3-B-7-Ni-treated wild-type mice ($n = 3$) and sarafotoxin-treated wild-type mice ($n = 4$). Asterisk, $P < 0.01$. **e**, Quantified pre-exercise (filled columns) and post-exercise (open columns) activity with and without treatment with PDE5A inhibitor, in *nNOS*-null ($n = 4$), MCKεSG/*Sgca*-null ($n = 4$) and *mdx* mice ($n = 6$). Asterisk, $P < 0.0001$. Pre-exercise and post-exercise vertical activity error bars are s.e.m.

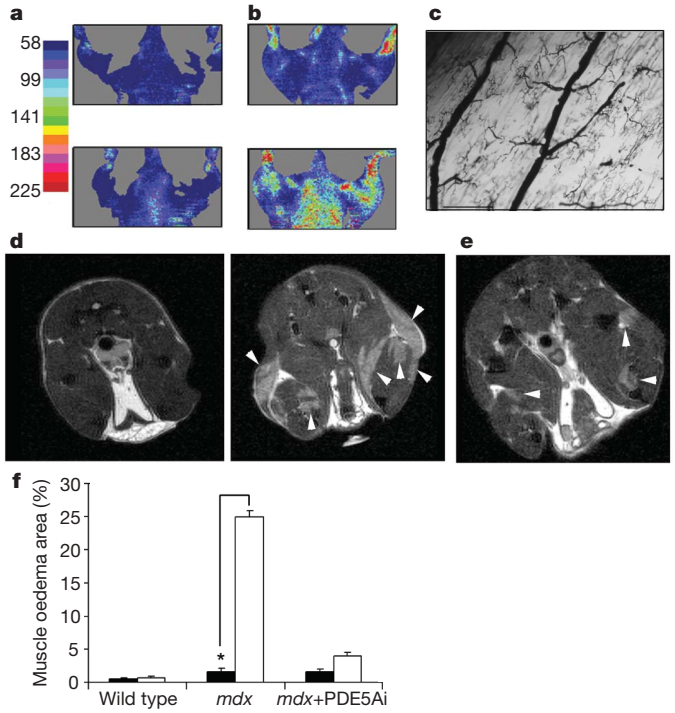

Figure 3 | Treatment with PDE5A inhibitor improves exercised-induced vasomodulation and decreases exercise-induced oedema in *mdx* mice. **a**, Representative images of coronal laser Doppler analysis of blood flow in *mdx* mice before (top) and after (bottom) exercise ($n = 3$). **b**, Coronal laser Doppler analysis of blood flow in *mdx* mice, before (top) and after (bottom) exercise, treated with PDE5A inhibitor before exercise ($n = 3$). **c**, Representative Microfil image of quadriceps skeletal muscle arteries after exercise from *mdx* mice treated with PDE5A inhibitor before exercise ($n = 3$; scale bar, 100 μm). **d**, **e**, Representative axial views, by magnetic resonance imaging, of *mdx* hindlimb muscles before (left) and after (right) exercise ($n = 5$) (**d**) and hindlimb muscles after exercise of *mdx* mice treated with PDE5A inhibitor before exercise ($n = 5$) (**e**). White arrowheads mark areas of increased water compartmentalization. **f**, Percentage muscle oedema area before (filled columns) and after (open columns) exercise, and with or without treatment with PDE5A inhibitor, in *mdx* mice compared with that of the wild type. (Wild type and *mdx*, $n = 3$; *mdx* plus PDE5A inhibitor, $n = 5$; error bars are s.e.m.) Asterisk, $P < 0.001$.

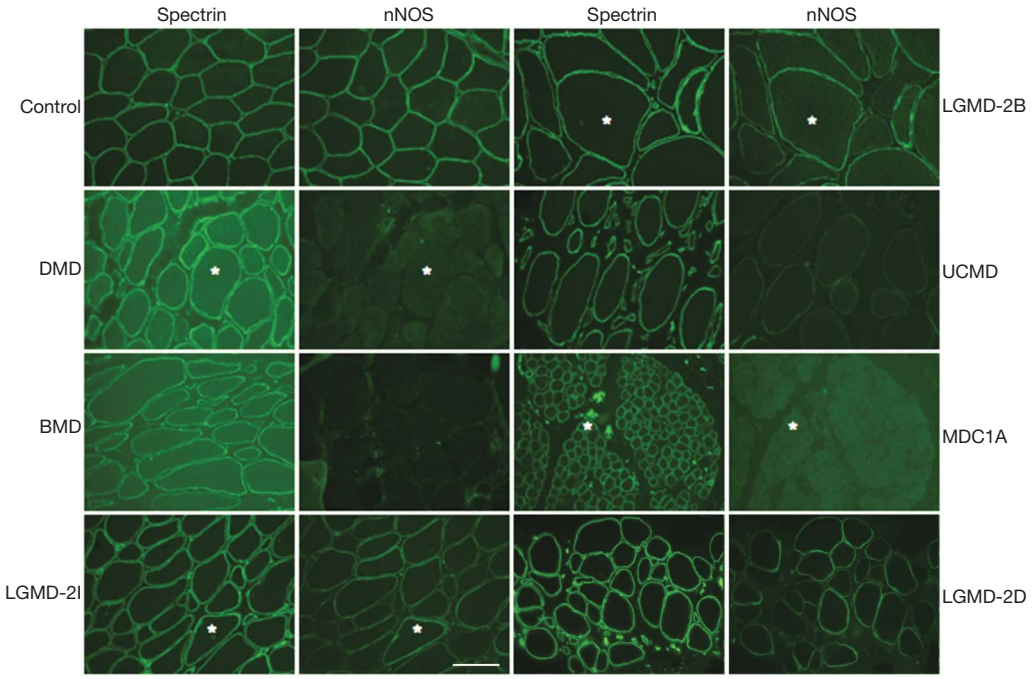

Figure 4 | nNOS levels in sarcolemma are decreased in human muscle diseases. Representative immunofluorescent staining in various human muscle diseases: primary dystrophinopathies, Duchenne and Becker muscular dystrophy (DMD and BMD, respectively); in several forms of limb-girdle muscular dystrophy (LGMD); in two congenital muscular dystrophies (CMD) caused by mutations in extracellular matrix proteins (Ullrich CMD (UCMD), collagen VI and merosin-deficient CMD (MDC1A). Asterisks mark the same muscle fibres in some of the adjacent panels. Scale bar, 100 μm.

Supplementary Fig. 8b). However, hindleg muscles of *mdx* mice consistently showed significant changes in tissue hydration after exercise (25.0 ± 2.45% (mean ± s.e.m.)) (Fig. 3d, f) that were indicative of exercise-induced muscle oedema. The water accumulation observed in the *mdx* muscles is probably due to a combination of the increased local resistance in the arterioles that feed the active leg muscles and of muscle fibre fragility and damage. We also consistently found that treatment with PDE5A inhibitor significantly decreased exercise-induced muscle oedema in *mdx* mice (3.99 ± 0.82% (mean ± s.e.m.); Fig. 3e, f). Overall, our data imply that treatment with PDE5A inhibitor can relieve the post-exercise inactivity by normalizing PDE activity, thereby allowing the available NO derived from muscle nNOS to signal for cGMP-dependent vasodilation in active muscle; treatment with PDE5A inhibitor decreases muscle damage in *mdx* mice by improving modulation of vascular activity in active muscle, thus preventing muscle oedema from exacerbating the muscle damage that occurs during the contraction of dystrophic muscle.

Because more than 60% of all patients with neuromuscular disease suffer from severe fatigue[2], we tested for nNOS localization to the sarcolemma in biopsies of patients representing different myopathic disorders (Fig. 4, Supplementary Fig. 9 and Supplementary Table 1). In most myopathic biopsies assessed, sarcolemma-localized nNOS was either reduced or not detected, implying that many myopathic disorders may share a mechanism that results in severe exercise-induced fatigue. Although increased fatigability inevitably occurs in patients with muscle weakness[1], our mouse data imply that the exercise-induced inactivity is distinct from muscle weakness and that loss of sarcolemma-localized nNOS leads to an exaggerated fatigue response to mild exercise.

Our mouse data show that decreased or mislocalized skeletal muscle nNOS exacerbates the fatigue experienced after mild exercise because the normal contraction-induced cGMP-dependent attenuation of local vasoconstriction fails to occur, and that this failure causes vascular narrowing in muscles after exercise. In addition, our data from *mdx* mice suggest that, as a result of nNOS mislocalization and increased PDE activity[10,18,21], signalling for increased vasodilation to active muscle is deficient, causing muscle oedema. This, in turn, contributes to increased muscle damage as well as profound post-exercise debility. Although the exact mechanism that leads to the inactivity after mild exercise has not been reduced to a single beginning and end pathway, our data suggest that contraction-induced cGMP-dependent attenuation of local vasoconstriction is pivotal in this mechanism. These findings could lead to a better understanding of muscle fatigue under other physiological conditions in which muscle nNOS expression, localization or activity is affected.

METHODS SUMMARY

Mouse models. Animal care and procedures were approved and performed in accordance with the standards set forth by the National Institutes of Health and the University of Iowa Animal Care and Use Committee.

Treadmill exercise and activity monitoring. Animals were mildly exercised with an adjustable variable-speed belt treadmill from AccuPacer. Activity based on ambulatory behaviour was assessed in an open-field test.

Received 16 January; accepted 29 August 2008.
Published online 26 October 2008.

1. Schillings, M. L. *et al.* Experienced and physiological fatigue in neuromuscular disorders. *Clin. Neurophysiol.* **118,** 292–300 (2007).
2. Zwarts, M. J., Bleijenberg, G. & van Engelen, B. G. Clinical neurophysiology of fatigue. *Clin. Neurophysiol.* doi:10.1016/j.clinph.2007.09.126 (2007).
3. Kalkman, J. S., Schillings, M. L., Zwarts, M. J., van Engelen, B. G. & Bleijenberg, G. The development of a model of fatigue in neuromuscular disorders: A longitudinal study. *J. Psychosom. Res.* **62,** 571–579 (2007).
4. Radley, H. G., De Luca, A., Lynch, G. S. & Grounds, M. D. Duchenne muscular dystrophy: focus on pharmaceutical and nutritional interventions. *Int. J. Biochem. Cell Biol.* **39,** 469–477 (2007).
5. Duclos, F. *et al.* Progressive muscular dystrophy in α-sarcoglycan-deficient mice. *J. Cell Biol.* **142,** 1461–1471 (1998).
6. Ozawa, E., Mizuno, Y., Hagiwara, Y., Sasaoka, T. & Yoshida, M. Molecular and cell biology of the sarcoglycan complex. *Muscle Nerve* **32,** 563–576 (2005).
7. Consolino, C. M. *et al.* Muscles of mice deficient in α-sarcoglycan maintain large masses and near control force values throughout the life span. *Physiol. Genomics* **22,** 244–256 (2005).
8. Yokoyama, T., Lisi, T. L., Moore, S. A. & Sluka, K. A. Muscle fatigue increases the probability of developing hyperalgesia in mice. *J. Pain* **8,** 692–699 (2007).

9. Harper, S. Q. *et al.* Modular flexibility of dystrophin: implications for gene therapy of Duchenne muscular dystrophy. *Nature Med.* **8,** 253–261 (2002).
10. Imamura, M., Mochizuki, Y., Engvall, E. & Takeda, S. I. ε-Sarcoglycan compensates for lack of α-sarcoglycan in a mouse model of limb-girdle muscular dystrophy. *Hum. Mol. Genet.* **14,** 775–783 (2005).
11. Phillips, B. A. & Mastaglia, F. L. Exercise therapy in patients with myopathy. *Curr. Opin. Neurol.* **13,** 547–552 (2000).
12. Torelli, S. *et al.* Absence of neuronal nitric oxide synthase (nNOS) as a pathological marker for the diagnosis of Becker muscular dystrophy with rod domain deletions. *Neuropathol. Appl. Neurobiol.* **30,** 540–545 (2004).
13. Judge, L. M., Haraguchiln, M. & Chamberlain, J. S. Dissecting the signaling and mechanical functions of the dystrophin–glycoprotein complex. *J. Cell Sci.* **119,** 1537–1546 (2006).
14. Thomas, G. D., Shaul, P. W., Yuhanna, I. S., Froehner, S. C. & Adams, M. E. Vasomodulation by skeletal muscle-derived nitric oxide requires α-syntrophin-mediated sarcolemmal localization of neuronal nitric oxide synthase. *Circ. Res.* **92,** 554–560 (2003).
15. Chao, D. S., Silvagno, F. & Bredt, D. S. Muscular dystrophy in *mdx* mice despite lack of neuronal nitric oxide synthase. *J. Neurochem.* **71,** 784–789 (1998).
16. Crosbie, R. H. *et al. mdx* muscle pathology is independent of nNOS perturbation. *Hum. Mol. Genet.* **7,** 823–829 (1998).
17. Suzuki, N. *et al.* NO production results in suspension-induced muscle atrophy through dislocation of neuronal NOS. *J. Clin. Invest.* **117,** 2468–2476 (2007).
18. Asai, A. *et al.* Primary role of functional ischemia, quantitative evidence for the two-hit mechanism, and phosphodiesterase-5 inhibitor therapy in mouse muscular dystrophy. *PLoS ONE* **2,** e806 (2007).
19. Huang, P. L. *et al.* Hypertension in mice lacking the gene for endothelial nitric oxide synthase. *Nature* **377,** 239–242 (1995).
20. Thomas, G. D. *et al.* Impaired metabolic modulation of α-adrenergic vasoconstriction in dystrophin-deficient skeletal muscle. *Proc. Natl Acad. Sci. USA* **95,** 15090–15095 (1998).
21. Bloom, T. J. Age-related alterations in cyclic nucleotide phosphodiesterase activity in dystrophic mouse leg muscle. *Can. J. Physiol. Pharmacol.* **83,** 1055–1060 (2005).
22. Bloom, T. J. Cyclic nucleotide phosphodiesterase isozymes expressed in mouse skeletal muscle. *Can. J. Physiol. Pharmacol.* **80,** 1132–1135 (2002).
23. Kass, D. A., Champion, H. C. & Beavo, J. A. Phosphodiesterase type 5: expanding roles in cardiovascular regulation. *Circ. Res.* **101,** 1084–1095 (2007).
24. Persson, J., Ekelund, U. & Grande, P. O. Endogenous nitric oxide reduces microvascular permeability and tissue oedema during exercise in cat skeletal muscle. *J. Vasc. Res.* **40,** 538–546 (2003).
25. Marden, F. A., Connolly, A. M., Siegel, M. J. & Rubin, D. A. Compositional analysis of muscle in boys with Duchenne muscular dystrophy using MR imaging. *Skeletal Radiol.* **34,** 140–148 (2005).

Supplementary Information is linked to the online version of the paper at www.nature.com/nature.

Acknowledgements We thank M. Anderson and M. Henry for comments, and M. M. Kilburg, K. Uppal, B. J. Steinmann and S. Watkins and members of the Campbell laboratory for scientific contributions. This work was supported in part by a Paul D. Wellstone Muscular Dystrophy Cooperative Research Center Grant. Y.M.K. was supported by grants from the University of Iowa Cardiovascular Interdisciplinary Research/ National Research Service Award (NRSA) Fellowship, from an individual NRSA Fellowship from the National Institute of Arthritis and Musculoskeletal and Skin Diseases, from the National Institutes of Health (NIH), and from a Senator Paul D. Wellstone Fellowship. E.P.R. was supported by a Muscular Dystrophy Association Development Grant. R.M.W. was supported by the NIH. K.P.C. is an investigator of the Howard Hughes Medical Institute.

Author Information Reprints and permissions information is available at www.nature.com/reprints. Correspondence and requests for materials should be addressed to K.P.C. (kevin-campbell@uiowa.edu).

ADDITIONAL METHODS

Mouse models. Mouse strains obtained from Jackson Laboratories: C57BL/6, C57BL/10, *mdx*/C57BL/10ScSn, *nNOS*-null, and *eNOS*-null. Microdystrophin/*mdx* mice were described previously[1, 2]. Mice were maintained at the University of Iowa Animal Care Unit in accordance with the institute's animal usage guidelines. We found that sarcolemmal nNOS in female C57BL/6 mice was less than or equal to that in their male counterparts, depending on the stage of the estrous cycle; since even ovariectomized rats[3] and ovariectomized mice lose sarcolemmal nNOS, we only tested males. All mice were 10 wks of age, unless otherwise stated. Genetically defined mice were randomized between cages to avoid bias and tested blindly. *Sgca*-null mice[4] were backcrossed to a C57BL/6 background (BC5). MCKεSG/*Sgca*-null mice were bred with the *Sgca*-null (BC5) line for 8 generations. EC-SOD mice were from J.D. Crapo's laboratory and expression was driven by the β-actin promoter; these mice were mated with *mdx* mice for two generations and tested. *Dtna*-null mice[5] were on a pure C57BL/6 background and were from Drs. R. Mark Grady and J.R. Sanes.

Exercise-activity assay. Mouse housing and exercise-activity rooms were under specific pathogen-free conditions. Since anesthesia causes alterations in blood glucose[6] as well as in the blood flow[7] to skeletal muscle, we designed our exercise-activity assay without anesthesia. Also, to reduce anxiety, which could potentially lead to increases in blood glucose, and to keep behavioral variables at a minimum, we tested mice that were not individually housed[8]. The same handler performed each assay. Mice were activity-monitored using the VersaMax Animal Activity Monitoring System from AccuScan Instruments, Inc. This system uses a grid of invisible infrared light beams that traverse the animal chamber front to back and left to right to monitor the position and movement of the mouse within an X-Y-Z plane. Activity was monitored over a 24 hour cycle to determine their most active time. All mice tested were synchronized to a shifted 12:12-hour light:dark cycle so that at the time of testing, the mice were behaviorally most active. Mice were acclimatized to the activity test room, which was on the same light:dark cycle, for at least an hour. Mice were tested in individual chambers in sets of 4, for 30 x 1 minute intervals pre- and immediately post-exercise, at the same time every day in the dark, in an isolated room, and with the same handler. Testing equipment was cleaned between each use to reduce mouse reactionary behavioral variables that could alter our results. Data collected was converted to a Microsoft Excel worksheet and all calculations were done within the Excel program. Zone map tracings were created by the AccuScan VersaMap-Zone mapping software where the X and Y plane represent the 2 dimensions of the activity chamber and the dots represent every time the mouse breaks the Z plane, registering vertical activity within the 30 minute time interval.

Animals were mildly exercised using an adjustable variable speed belt treadmill from AccuPacer (AP4M-MGAG, AccuScan Instruments, Inc.), down a 15° grade at 15 mpm for 10 minutes with acclimatization at 3 mpm for 5 minutes.

Antibodies. The nNOS antibody used for immunoblots and immunofluorescence was an affinity purified polyclonal antibody[9]. Antibodies for inflammation included: I-A^b MHC class II-conjugated to FITC and F4/80 conjugated to Alex Fluor® 647, both from

Invitrogen. For an atrophy marker, SC-71 antibody (ATCC) against myosin heavy chain 2A was used. For hypoxia and oxidative stress, polyclonal antibodies against HIF-1α (R&D Systems) and nitrotyrosine (Upstate), and Hypoxyprobe-1™ Mab1 conjugated to FITC (Chemicon® International) were used.

Immunoblotting analysis. Tissue for immunoblotting came from whole muscle and crude skeletal muscle membranes were prepared as follows: 1-3 g fresh hind leg skeletal muscle was homogenized in 7.5x volumes homogenization buffer (20 mM $Na_4P_2O_7$, 20 mM NaH_2PO_4, 1 mM $MgCl_2$, 0.303 M sucrose, 0.5 mM EDTA, pH 7.1 with 5 ug/ml Aprotinin and Leupeptin, 0.5 ug/ml Pepstatin A, 0.23 mM PMSF, 0.64 mM Benzamidine, and 2 uM Calpain inhibitor I and Calpeptin), then centrifuged 14k x g_{max}; supernatants were centrifuged 30k x g_{max}, after which pellets were resuspended in homogenization buffer. Homogenates and crude skeletal muscle membranes were prepared from different mouse models, run on SDS-PAGE and transferred to PVDF (Immobilon-P) transfer membranes for immunoblotting[10]. All immunoblotting was done by chemiluminescent detection using the Alpha Innotech imaging system.

Immunofluorescence analysis. Immunofluorescence staining for nNOS was performed on 7 μm transverse cryo muscle sections as described previously[9]. For patient biopsies, immunofluorescence staining was performed on serial cryosections; both anti-spectrin and anti-nNOS antibodies were purchased from Novocastra. For hypoxia analysis +/- exercise, Hypoxyprobe™ was injected 45 min before exercise.

Microfil® analysis of skeletal muscle vessels. Microfil® MV-130 Red (Flow Tech, Inc) was mixed according to manufacturer's instructions and perfused into the mouse aorta pre- or post-exercise at 100 mm Hg. After polymerization and clearing of skeletal muscles, vessels were imaged.

Tissue blood-flow mapping. The MoorLDI™ system using near infra-red wavelength laser (1.0 mm beam, 2.5 mW) doppler imaging without contrast was used to generate a color coded map of blood flow on a CCD camera at 72 x 582 pixel resolution. Range was at 20 cm distance in an area 5.1 cm x 4.2 cm at 182 x 152 resolution and scan speed of 4 ms/pixel.

Serum Creatine Kinase Assays. Blood for quantitative, kinetic determination of serum creatine kinase activity was collected either after the pre-exercise activity analysis or 2 hours post-exercise by mouse tail vein bleeds, using a Sarstedt microvette CB 300, from non-anesthetized restrained mice. Red cells were pelleted by centrifugation at 10,000 rpm for 4 minutes and serum was separated, collected and analyzed immediately without freezing. Serum creatine kinase assays were done with an enzyme-coupled assay reagent kit (Stanbio Laboratory) according to manufacturer's instructions. Absorbance at 340 nm was measure every 30 sec for 2 min at 37°C so that changes in enzyme activity could be calculated. Data were transferred to and calculated in a Microsoft Excel spreadsheet.

Contractile properties. Contractile properties were measured *in vitro* on extensor digitorum longus (EDL), soleus, or diaphragm muscles strips from C57BL/6, *mdx*,

MCKεSG/*Sgca*-null, MCKεSG, *Sgca*-null, or *nNOS*-null mice. Mice were anesthetized by an intraperitoneal injection (I.P.) of 2% avertin (0.0015 ml/g body weight). Supplemental injections were administered to maintain an anesthesia level that prevented responses to tactile stimuli. Intact muscles or DPM strips were removed from each mouse after the mice were euthanized by an overdose of avertin, and the thoracic cavity was opened. Muscles were immersed in an oxygenated bath (95% O_2, 5% CO_2) that contained Ringer's solution (pH 7.4) at 25°C. For each muscle, one tendon was tied securely with a 4-0 or 6-0 suture to a force transducer (one end), and a servo motor (other end). Using twitches with pulse duration of 0.2 ms, the voltage or current of stimulation was increased to achieve a maximum twitch and then increased slightly. Twitches were then used to adjust the muscle length to the optimum length for force development (L_o). The muscle length was set at L_o , and EDL muscles were stimulated for 300 ms, and soleus and DPM muscles for 900 ms. Stimulation frequency was increased until the force reached a plateau at maximum isometric tetanic force (P_o).

For C57BL/6, *mdx*, MCKεSG/*Sgca*-null, MCKεSG, *Sgca*-null mice, the susceptibility to contraction-induced injury was measured during two lengthening contractions, with the contractions separated by a rest interval of 10 s. Each contraction was initiated with the quiescent muscle set at L_o, and then a plateau at maximum force was produced by stimulating EDL muscles at a frequency of ~150 Hz for 150 ms and soleus and DPM muscles at ~120 Hz for 200 ms. While generating maximum force, the muscles were stretched through a 30% strain at a velocity of 1 Lf/s, and then returned to L_o. A measurement of P_o was made one minute later. Based on measurements of muscle mass, muscle length, fiber length, and P_o, the total fiber cross-sectional area and specific P_o (kN/m2) were calculated[1, 11]. The data were analyzed by an analysis of variance (ANOVA). When the overall F-ratio for the ANOVA was significant, the differences between individual group means were determined by a single t-test. Significance was set *a priori* at $P < 0.05$. Data are expressed as mean ± SEM.

Drug treatments. Timing and dosing of deflazacort was based on previous literature on *mdx* mice treated with deflazacort showing beneficial effects on *mdx* muscle pathology[12-15]. The steroidal anti-inflammatory Deflazacort (Axxora® Platform) was resuspended in DMSO at 36 mg/ml and then diluted 1:100 in 0.9% saline immediately prior to I.P. injection at 1.5 mg/kg/day for acute and 1.2 mg/kg/day for the 3-week chronic treatment. Timing and dosing of ibuprofen (Alpharma, Inc) was based on veterinary formularies for anti-inflammatory and analgesic doses and previous literature[16, 17]. Ibuprofen was in suspension and delivered orally at 50 mg/kg/day.

The nNOS inhibitor 3-bromo-7-nitroindazole (3-B-7-Ni) (Cayman Chemical) or the endothelin receptor type 1b agonist, sarafotoxin 6c (a vasoconstrictor peptide, Alexis Biochemicals), was resuspended in DMSO at 100 mg/ml and 1 mg/ml, respectively. 3-B-7-Ni was diluted 1:10 in sunflower oil and immediately injected at 20 mg/kg I.P. Sarafotoxin 6c was diluted 1:1000 in 0.9% saline and immediately injected at 5 ug/kg I.P.

In determining the dosage of PDE5A inhibitor, we wanted our dose of PDE5A inhibitor to give a good exposure to PDE5A, so we took into account the following points: a dose of 100 mg/kg/day will give a mean free plasma concentration of 10.4 nM[18-20] (the IC_{50} of sildenafil at PDE5A is 5-10 nM[19] thus 100 mg/kg/day is at the IC_{50} for sildenafil at PDE5A), PDE5 activity is elevated 2-6x in mouse leg muscle extracts from *mdx* mice[21],

and food-drug interactions reducing the rate of absorption and extent of systemic exposure for PDE5A inhibitors[18]. Doses of 100, 300, and 500 mg/kg/day were tested on *mdx* mice and 300 mg/kg/day gave the best response (see Figure S7d). Assuming linear pharmacokinetics from 100-300 mg/kg/day, 300 mg/kg/day will produce approximately a plasma concentration of 30 nM, exceeding the IC_{50} by 3-6 fold, inhibiting more than 50% of the enzyme activity. Therefore, for acute tadalafil (Kemprotec) treatment, tadalafil was given orally by gavage at 300 mg/kg the day before and the day of the exercise-activity protocol to ensure that the mice received one full day of inhibitor dosage before the exercise-activity protocol. For acute sildenafil citrate (Pfizer) treatment, sildenafil was given orally by mixing the drug into water softened rodent gruel (2019 Teklad global 19% protein rodent chow; 4-6 g/day). Mice were supplemented with normal chow (7013 NIH-31 modified diet) to ensure *ad libitum* feeding. For K_{ATP} channel agonists, stocks at 100 mg/ml of Minoxidil (Sigma) and pinacidil (Alexis Biochemicals) were resuspended in DMSO, and nicorandil (SynFine Research) was resuspended in water. Each drug was diluted in 0.9% saline immediately before i.p. injection, at 0.8 mg/kg in the case of minoxidil and pinacidil or 0.1 mg/kg in the case of nicorandil. L-NAME was given orally by gavage at 100 mg/kg in 0.9% saline the day before and the day of the exercise-activity protocol. Superoxide dismutase (Sigma) was given by i.v. at 1000 U/mouse. Tempol (Alexis Biochemicals) was delivered by i.p. at 260 mg/kg.

All agents were administered 30 minutes prior to exercise-activity analysis unless otherwise stated.

Magnetic resonance imaging (MRI). MRI was performed using a Varian Unity/Inova 4.7 T small-bore MRI system (Varian Inc., Palo Alto, CA). The acquisition consisted of a T2-weighted fast spin-echo sequence (TR/TE = 5000/48 ms) with in-plane resolution of 0.11 mm x 0.22 mm and slice thickness of 0.6 mm acquired in the axial plane. Imaging of mice was +/- exercise. For imaging, mice were anesthetized with an i.p. injection of ketamine/xylazine (87.5 mg/kg and 12.5 mg/kg, respectively). If with exercise, imaging started 30 minutes post-exercise. 4 *mdx* mice were imaged for pre-exercise and 7 *mdx* mice were imaged for post-exercise and 5 *mdx* were treated with PDE5A inhibitor. Three mice were examined for other sets. Measurements to determine percent muscle edema were done with Image-ProPlus6.0 Software. Axial or coronal muscle areas were measured and fat and cartilage were subtracted. Total areas of edema were measured within the same slice and divided by the resultant axial muscle area and multiplied by 100 to get percent muscle edema area for each mouse tested (Fig. 3g). The middle axial and coronal slices were used for this quantitation as these slices gave the greatest viewable muscle area per scan. Axial and coronal calculations gave similar and consistent percent muscle edema areas.

Statistical analysis. Unless otherwise stated, the data were calculated according to an analysis of variance. *P*-value calculations were made between genetically defined mouse models and their wild-type counterparts or between treated and untreated mice using the Kruskal-Wallis One Way Analysis on Ranks. Data are expressed as mean ± SEM.

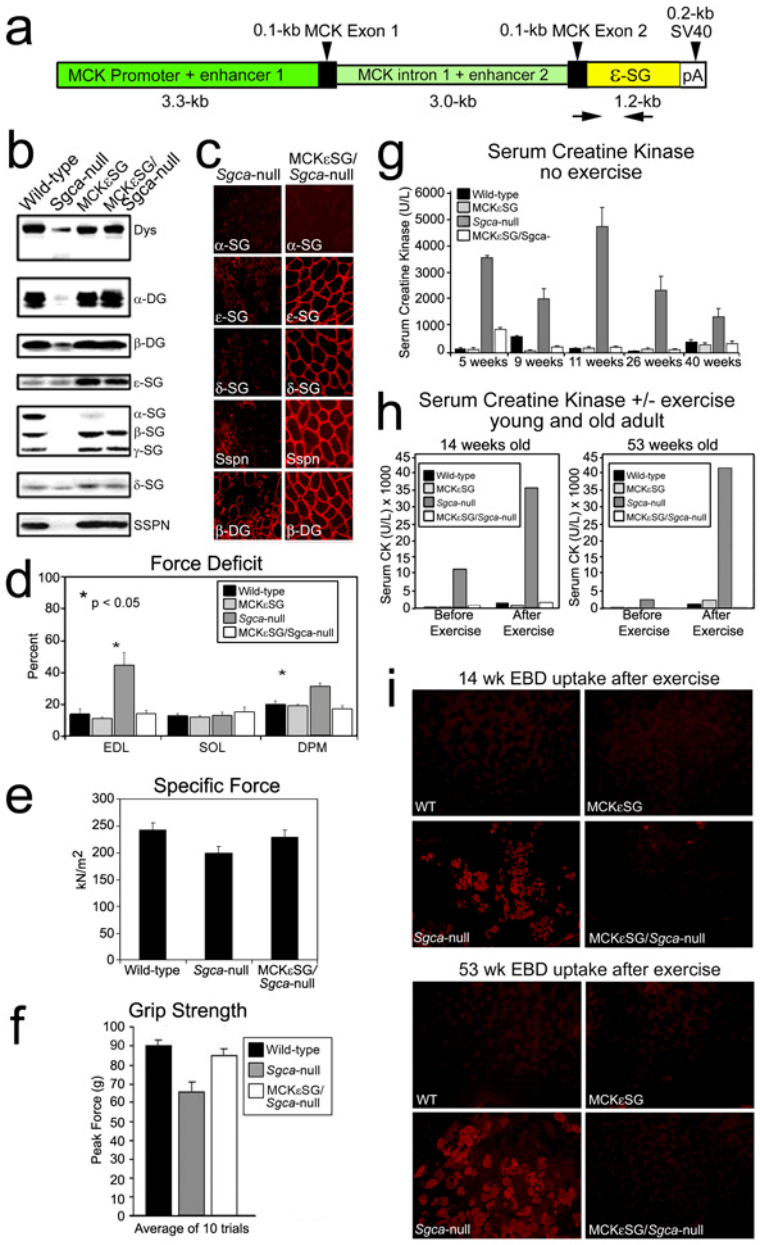

Figure S1 | Overexpression of ε-sarcoglycan in striated muscle of *Sgca*-null mice restores the DGC and normal muscle function. **a**, The mouse muscle creatine kinase promoter was used to drive transgenic expression of a human ε-sarcoglycan transgene in mice. Arrows indicate positions of primers used for genotyping. **b**, Immunoblotting for structural DGC components showed a complete recovery of the DGC in crude muscle membrane preparations from *Sgca*-null mice in which the ε-sarcoglycan transgene was expressed. Littermate wild-type, *Sgca*-null, and MCKεSG mice were used for a comparison of expression levels. **c**, Immunofluorescence detection of α-, ε-, δ-sarcoglycan, sarcospan, and β-dystroglycan in littermate 5-week old *Sgca*-null and MCKεSG/*Sgca*-null mouse quadriceps showing restoration of the sarcoglycans and sarcospan to the

sarcolemma, due to the expression of the ε-sarcoglycan transgene. Detection of β-dystroglycan was used as a control for membrane staining. **d**, Force deficit measurements of extensor digitorum longus (EDL), soleus, and diaphragm (DPM) muscles. All tests were performed on each of the 4 mouse strains with n=4 for each muscle of each strain. **e**, *In vitro* specific force measurements comparing wild-type, *Sgca*-null and MCKεSG/*Sgca*-null EDL muscles. **f**, Whole-mouse-grip strength force measurement comparing wild-type, *Sgca*-null and MCKεSG/*Sgca*-null forearm strength. **g**, Serum CK levels in unexercised mice, measured at different time points up to 40 weeks of age, showed MCKεSG/*Sgca*-null mice to have low CK levels that were similar to those of their littermate wild-type and MCKεSG controls, and much lower than those of *Sgca*-null littermate controls. **h**, Comparison of serum CK levels in 14- and 53-week old littermate wild-type, MCKεSG, *Sgca*-null, and MCKεSG/*Sgca*-null mice before and after exercise. **i**, Images of quadriceps muscle from each genotype, examined for Evans blue dye uptake, which indicates muscle fiber damage. (Error bars are S.E.M.)

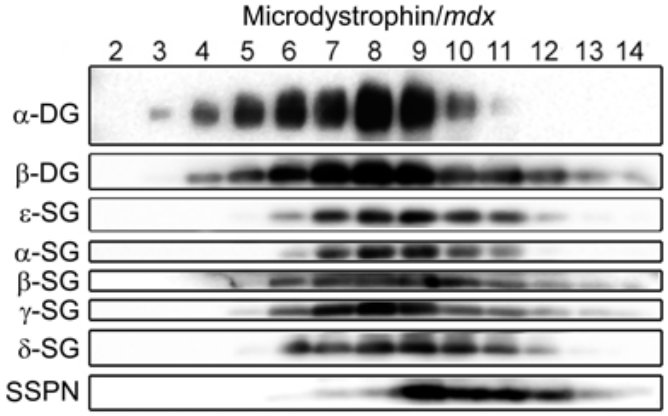

Figure S2 | Microdystrophin(udys)/*mdx* skeletal muscle DGC is intact. A sucrose density gradient of skeletal muscle DGC from microdystrophin/*mdx* mice, showing a structurally intact DGC – α- and β-dystroglycan (α-DG and β-DG), α/ε-sarcoglycan (α/ε-, β-, γ-, and δ-SG), and sarcospan (SSPN). In *mdx* mice, the DGC structural components are dispersed through the sucrose gradient[22].

Microdystrophin/*mdx* mice show restoration of the structural DGC proteins to the sarcolemma, with contractility returning to the levels seen in wild-type mice[1] but, as we show in Figure 1e, without restoration of nNOS to the sarcolemma. We also show in Figure 1e that microdystrophin/*mdx* mice have excessive inactivity after mild exercise, despite contractility being normal.

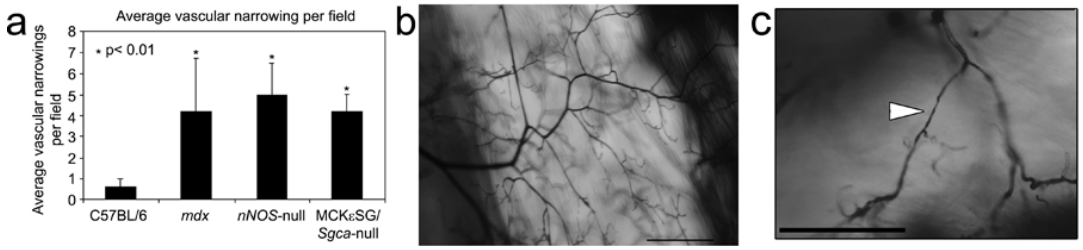

Figure S3 | Vascular narrowings after exercise. **a**, Skeletal muscle vascular narrowings were averaged per field after exercise and compared to wild-type mice. After exercise, C57BL/6 mice have increased capillary perfusion and little to no vascular narrowings (**b**) whereas *mdx* (**c**), MCKεSG/*Sgca*-null, and *nNOS*-null mice do not (see Figure 1g and 2c). Each Microfil® image is a representative view of skeletal muscle vessels post-exercise. Arrowhead indicates narrowing. (Error bars = SEM, scale bar = 100 μm)

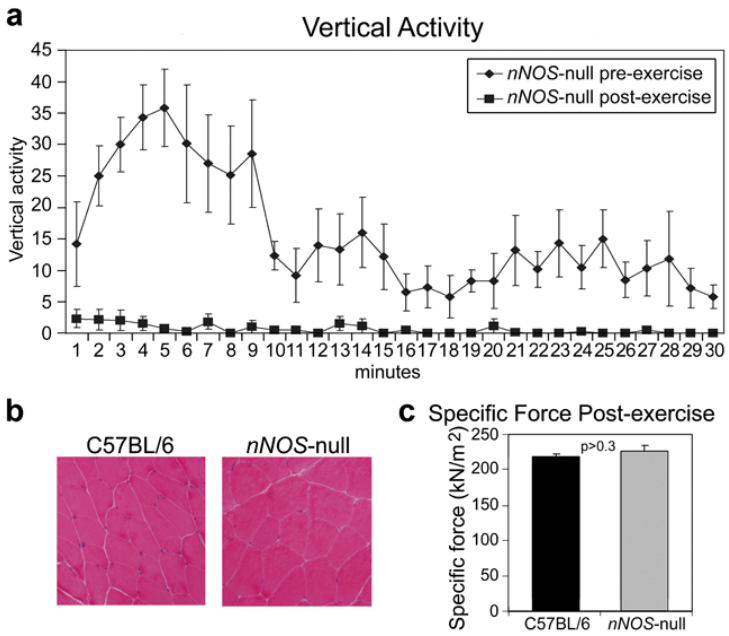

Figure S4 | *nNOS*-null mice after mild exercise. a, Charting of vertical activity for 30 minutes pre- and post-exercise showing that following a light bout of activity, the vertical activity in *nNOS*-null mice is extremely low throughout the entire 30 minute analysis. (n=4 for each). (Error bars are S.E.M.). **b**, Comparison of hematoxylin and eosin staining of quadriceps muscle sections from C57BL/6 and *nNOS*-null mice (n=6 for each) showing no signs of muscle pathology. **c**, Contractility comparison measuring specific force after mild exercise in C57BL/6 and *nNOS*-null EDL muscles (n=5 for each).

The exaggerated fatigue response to mild exercise is not muscle weakness. Evidence from mouse models demonstrates that reduced sarcolemmal nNOS does not affect muscle contractility: microdystrophin/*mdx*[1], MCKεSG/*Sgca*-null, and α1-*syntrophin*-null[23] mice have mislocalized nNOS but this does not influence contractile properties. In addition, *nNOS*-null muscles produce force comparable to, or even greater than, the force generated by wild-type muscle at different oxygen tensions[24]. To further test if loss of nNOS affects contractility, we exercised a set of *nNOS*-null mice, waited 10 minutes, which was within

the 30 minute time interval we used to assess the fatigue response after mild exercise (Supplemental Fig. S3), and put them on the treadmill again. The mice were able to run the full running protocol again indicating that they were still capable of performing physical activity and that the activity was not exhaustive. Our *nNOS*-null mouse data show that loss of nNOS-derived NO signaling leads to prolonged exercise-induced inactivity similar to that identified in our dystrophic and rescue mouse models.

In the mouse models with the fatigue response to mild exercise, full activity returned, and vascular narrowing were not present 4 hours after exercise indicating that the vascular narrowing as well as loss of activity post-exercise is not sustained. Vascular narrowings and the fatigue response occur again upon re-exercising of mice.

Non-selective NOS inhibitor data are consistent with our results from the treatment of wild-type mice with the relatively specific nNOS inhibitor 3-bromo-7-nitroindazole: treatment of wild-type mice with L-NNA prevents adequate exercise-induced hyperemia and limits exercise capacity during exhaustive treadmill running[25]; treatment of wild-type and *mdx* mice with L-NAME increases mean arterial pressure and decreases femoral blood flow velocity and vascular conductance[26]; L-NAME treatment severely reduces walking speed in rats[27], and local intra-arterial infusion of L-NMMA into human forearm reduces resting blood flow and a transient systemic increase in blood pressure[28]. We found that treatment of wild-type mice with L-NAME reduced post-exercise activity to levels similar to those in *nNOS*-null mice post-exercise, and that treatment of dystrophic or *nNOS*-null mice with L-NAME reduced the activity post-exercise even more, in fact preventing Microfil® from circulating sufficiently for images to be taken (data not shown). The L-NAME results are also consistent with our sarafotoxin 6c treatment of wild-type mouse data. In addition, the NOS inhibitor and sarafotoxin data are consistent with the fact that deflazacort treatment of *mdx* mice did not ameliorate inactivity post-exercise as glucocorticoids reduce inflammation by causing vasoconstriction to reduce blood flow and thus reducing permeability between the endothelial cells[29].

The exaggerated fatigue response to mild exercise is not due to oxidative stress, inflammation, or atrophy. To test the possibility that an inhibition of mitochondrial respiration inhibition causes the observed post-exercise inactivity, we tested *mdx* mice treated with superoxide dismutase (SOD) or *mdx* mice overexpressing the extracellular superoxide dismutase (under the β-actin promoter) in our exercise activity assay. We found that neither method of SOD exposure had an effect on the exaggerated fatigue response to mild exercise. In addition, since reactive oxygen species (ROS) increases the protein nitrosylation, we treated *mdx* mice with Tempol, a water-soluble, membrane permeable scavenger of superoxide anions that also reduces hydroxyl radical formation, and found that the drug had no effect on the exaggerated fatigue response in *mdx* mice. Furthermore, immunohistochemistry for nitrotyrosine in muscle sections of wild-type, rescue, or *nNOS*-null mice showed no changes +/- exercise.

We next probed for the expression of HIF-1α, an oxygen-dependent transcription activator that accumulates during oxidative stress, on skeletal muscle sections and on immunoblots of skeletal muscle homogenates, in wild-type, *mdx*, rescue, and *nNOS*-null mice before and after mild exercise, and did not detect any changes compared to levels in wild-type muscle. We also examined tissue hypoxia +/- exercise in wild-type, rescue, and

nNOS-null mouse models by injecting Hypoxyprobe™-1 and probed for hypoxyprobe adducts. We did not find signs of skeletal muscle hypoxia after the mild exercise.

On muscle sections of the non-dystrophic mouse models that displayed the exaggerated fatigue response, we probed for inflammation using I-A^b MHC class II and F4/80, and did not detect inflammation. To test for atrophy, we probed for myosin heavy chain 2A, and did not detect any signs of atrophy.

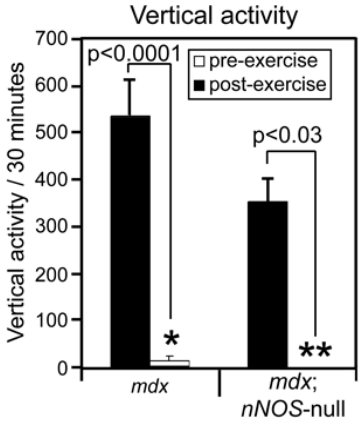

Figure S5 | *mdx*;*nNOS*-null mice and vertical activity. The exercise-induced vascular effect suggests that if nNOS were genetically deleted in a muscular dystrophy mouse model, the exercise-induced fatigue would be more significant. We tested this hypothesis by breeding the *mdx* and *nNOS*-null mice and analyzing the resulting *mdx*;*nNOS*-null mice in our exercise-activity assay. We found that the *mdx*;*nNOS*-null mice (n=4) had even less vertical activity pre- and post-exercise than their *mdx* littermates (*mdx*;$nNOS^{+/-}$ or *mdx*;$nNOS^{+/+}$)(n=7).

Loss of nNOS in *mdx* mice does not exacerbate muscle damage but will increase the exaggerated fatigue response to mild exercise. Comparative analyses of muscle pathology in *mdx*/*nNOS*-null mice versus *mdx* mice have led to the conclusion that *mdx* dystrophic pathology is independent of nNOS perturbation[9, 30]. However, fatigue was not analyzed in the *mdx*/*nNOS*-null mouse studies, and these mice were not challenged with exercise to test the repercussions of complete loss of nNOS in *mdx* muscle. On the other hand, NOS-Tg/*mdx* mice, which overexpress nNOS in *mdx* muscle, showed an amelioration of common indices of muscle pathology, due to reduced inflammation and membrane injury[31]. These mice, however, in spite of a 50-fold increase in nNOS protein in transgenic muscle, have only ~0.2 fold increase in NO production. This finding is reminiscent of the up-regulation of nNOS in DMD myofibers, which is accompanied by low NO levels[32]. The low NO production in NOS-Tg/*mdx* mice was attributed to possible increased expression of NOS inhibitors. However, this study did not confirm the localization of the overproduced nNOS protein, analyze fatigue, or challenge the NOS-Tg/*mdx* mice to analyze the effects of the 50-fold increase in nNOS expression in *mdx* mice.

Our muscle nNOS data are consistent with recent evidence showing that a structurally intact DGC in smooth muscle only partially restores α-adrenergic vasoregulation in *mdx* hindimbs[21], suggesting an extrinsic vascular contribution to vasomodulation. Importantly, we only see the vascular constrictions in the skeletal muscle

vasculature post-exercise in the *mdx*, *Sgca*-null, *nNOS*-null, and rescue mice. We did not detect vascular narrowing in other organs.

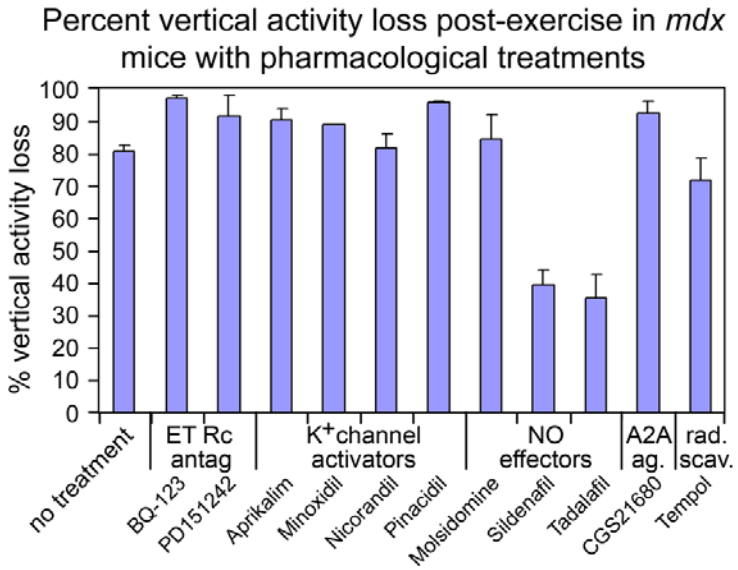

Figure S6 | Percent vertical activity loss post-exercise in *mdx* mice treated with different classes of pharmacological vasodilators. The loss of post-exercise vertical activity in *mdx* mice was quantified with and without treatment with various classes of vasodilators. The drugs tested were: ET_a receptor antagonists BQ-123 (0.1 mg/kg, n=3), and PD151242 (25 ug/mouse, n=4); the potassium channel activators Aprikalim (400 uM/mouse, n=4), Minoxidil (0.8 mg/kg, n=2), Nicorandil (0.1 mg/kg, n=2), and Pinacidil (0.8 mg/kg, n=2); the NO level activators Molsidomine (125 ug/mouse, n=4), Sildenafil (300 mg/kg, n=4), and Tadalafil (300 mg/kg, n=6) (note sildenafil and tadalafil affect cGMP levels, downstream of NO); the adenosine 2A receptor antagonist CGS21680 (1 ug/kg, n=2); and the superoxide scavenger Tempol (260 mg/kg, n=4). Untreated control mice for each drug class were pooled, resulting in n=34. Error bars are S.E.M.

The vasodilators bypass the nNOS-NO-cGMP mechanism and stimulate general vasodilation. While this would prevent vasoconstrictions like those seen with verapamil in sarcoglycanopathy mouse models[33], the bypass also eliminates the mechanism of nNOS stimulation by muscle contraction. Thus, the animals become hypotensive upon exercise and more inactive. For example: mice treated with minoxidil have catecholamines released into their bloodstream – a baroreflex-mediated response to low blood pressure[34]; nicorandil dilates peripheral and coronary resistance arterioles, systemic veins, and epicardial coronary arteries, thus significantly reducing blood pressure in mammals[35], and pinacidil decreases mean arterial pressure in wild-type mice[36].

Our data show that the exercise-induced prolonged fatigue response is alleviated by PDE5A inhibitor treatment, indicating that the effect we see is due to cGMP, which acts downstream of NO production. Downstream effects of low, physiological levels of NO (e.g. mitochondrial biogenesis and vasodilation) are cGMP-dependent, whereas downstream effects of high (pathological) NO levels (e.g. generation of reactive oxygen species and nitrosylation of proteins, lipids, and DNA) are cGMP-independent.[37]

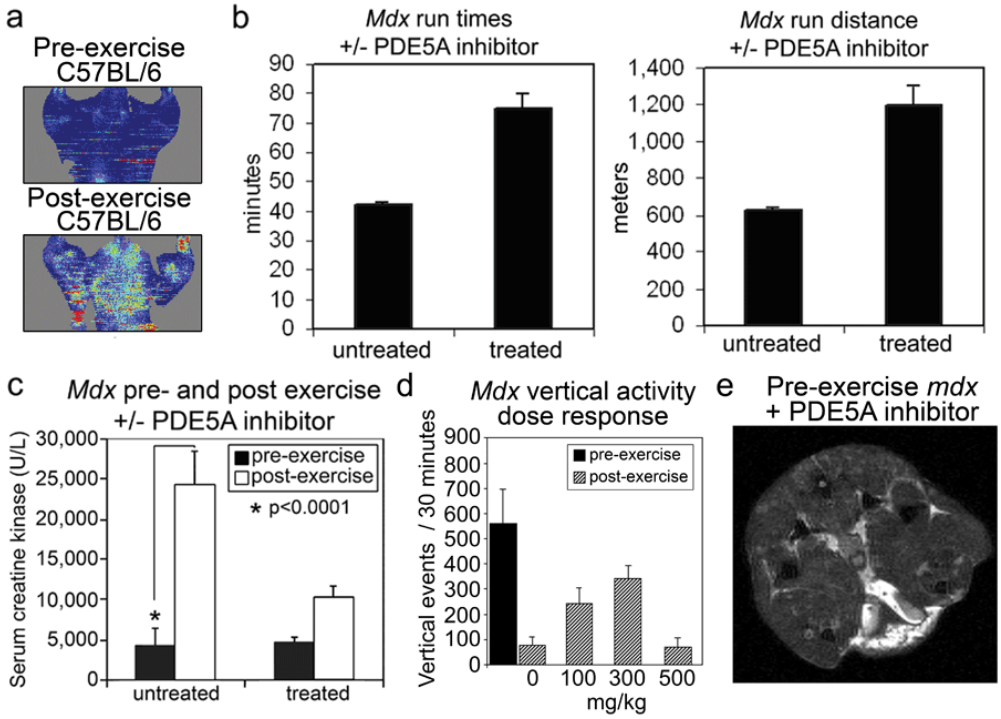

Figure S7 | PDE5A inhibitor treatment. a, Representative images of coronal Laser Doppler analysis of blood flow from C57BL/6 mice pre- and post-exercise (compare with Fig. 3a-b), b, *Mdx* mouse run times and run distances +/- PDE5A inhibitor treatment. **c**, *Mdx* pre- and post-exercise serum creatine kinase levels +/- PDE5A inhibitor treatment. (n=6 and error bars are S.E.M.) **d**, *Mdx* dose-vertical activity response curve to PDE5A inhibitor. (untreated n=6, 100 mg/kg n=3, 300 mg/kg n=6, 500 mg/kg n=3, error bars are S.E.M.), **e**, representative axial MRI view of pre-exercised *mdx* + PDE5A inhibitor.

Consistent with PDE5A inhibitor treatment attenuating muscle damage in *mdx* mice[21], we found that this treatment also reduced the rise in post-exercise serum creatine kinase and increased the time and distance of running of the *mdx* mice tested.

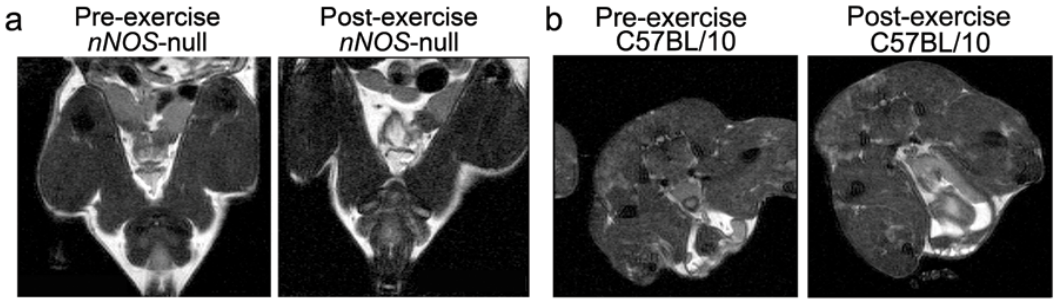

Figure S8 | No edema pre- and post-exercise in representative MRI views. **a**, Coronal views of *nNOS*-null hind-legs pre- and post-exercise (n=3), **b**, Axial views of C57BL/10 hind-legs (n=3) (0.70% +/- 0.50) (Compare to Fig. 3d-f),

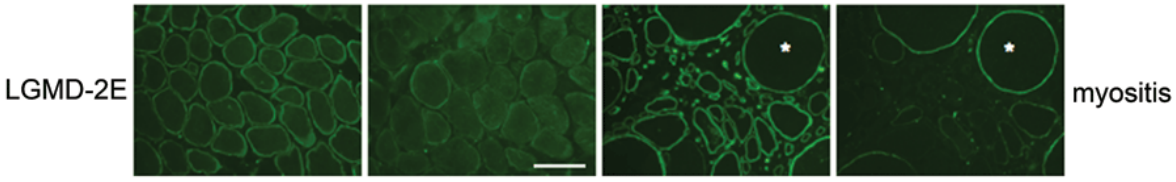

Figure S9 | nNOS is reduced in human muscle diseases. Additional example of a limb-girdle muscular dystrophy (LGMD-2E) and a non-dystrophic myopathy like polymyositis (myositis). Asterisks mark the same muscle fiber in some of the adjacent panels. (Compare to Fig. 4) (Scale bar = 100 um)

Table 1. Summary of the 425 human muscular biopsies stained for nNOS.

Disease	nNOS-negative	nNOS-reduced	nNOS-normal	Total cases stained
DMD	27	0	0	27
BMD	20	10	0	30
DMD carriers	Mosaic of negative and positive fibers			4
CMD/LGMD (POMT1, POMT2, POMGnT1, FKTN)	2	8	0	10
Other dystroglycanopathies not genetically defined	7	76	8	91
LGMD-2A	0	0	1	1
LGMD-2B	0	10	2	12
LGMD-2D	0	3	0	3
LGMD-2E	0	2	0	2
LGMD-2I	0	9	1	10
Other SG (includes three 2C cases)	0	6	0	6
UCMD	3	21	1	25
MDC1A	1	3	1	5
Myositis	2	6	0	8
Autophagic vacuolar myopathy	0	5	0	5
Myopathies w/o specific protein deficiencies	0	100	86	186

METHODS

Construction of transgene, transgenic mice, and MCKεSG/*Sgca*-null rescue mice. To direct skeletal and cardiac muscle-specific expression of ε-sarcoglycan in mice, an MCKεSGpA transgene was constructed: a 5' blunt-ended *Cla*I–3' *Xho*I fragment of the murine muscle-specific creatine kinase (MCK) 6.5-kb promoter/enhancer[38], was ligated into pGem7Zf(+) (Promega) 5' blunt-ended *Aat*II–*Xho*I sites. The full-length human ε-sarcoglycan cDNA (human and mouse ε-sarcoglycan are 96% identical) was PCR synthesized from a human skeletal muscle cDNA library (Clontech) and engineered with 5' *Xho*I–3' *Kpn*I sites then ligated downstream of the MCK promoter. An SV40 polyadenylation signal was PCR engineered with 5' *Kpn*I–3' HindIII/NruI/SacI linker and the *Kpn*I-*Sac*I fragment was ligated downstream of the ε-sarcoglycan coding region. All constructs were confirmed by DNA sequencing by the University of Iowa DNA Facility. The MCKεSGpA *EcoR*V–*Nru*I 7,986-bp transgene was microinjected by the University of Iowa Transgenic Animal Facility. Founder mice were identified, genotyped, and confirmed by PCR reactions of mouse genomic DNA isolated from tail or ear-snips[39]. Injection of the transgene yielded 3 independent germ line-transmitting founders, which were backcrossed to the C57BL/6 background to generate stable MCKεSG transgenic lines, and offspring were subsequently genotyped by PCR. Skeletal muscles from subsequent generations of transgenic mice were analyzed by SDS-PAGE to check for consistent expression of the transgene. MCKεSG/*Sgca*-null mice were generated by two rounds of breeding with *Sgca*-null mice[40] on a congenic C57BL/6 background. Offspring were PCR-genotyped for transmission of the transgene and loss of the corresponding allele.

Immunoblotting, immunofluorescence and histological analysis. Antibodies for immunoblots were MANDRA1 (dystrophin, Sigma-Aldrich), IIH6 (α-dystroglycan)[41], Rabbit 83 (β-dystroglycan)[42], Rabbit 229 (δ-sarcoglycan)[43], and Rabbit 256 (sarcospan)[44]. Monoclonal antibodies Ad1/20A6 (α-sarcoglycan), βSarc1/5B1 (β-sarcoglycan), and 35DAG/21B5 (γ-sarcoglycan) were generated in collaboration with L.V.B. Anderson (Newcastle General Hospital, Newcastle upon Tyne, UK). For the ε-sarcoglycan antibody (Rabbit 284), rabbit polyclonal antibodies were generated in New Zealand white rabbits intramuscularly and subcutaneously injected with a C-terminal mouse ε-sarcoglycan peptide (C-QTQIPQPQTTGKWYP) covalently linked to BSA. Antibody specificity was verified by competition experiments with the corresponding peptide on immunoblots. KCl-washed skeletal muscle membranes were prepared and immunoblot analysis was performed as described previously[10]. Immunofluorescence was performed on 7-μm transverse cryo sections as previously described[4]. Evans blue dye injections and exercise experiments were performed as described previously[4, 45].

Acknowledgements for supporting online material
Contractile properties (Supporting online material) were measured in the Contractility Core of Nathan Shock Center (J.A.F.).

References for supplementary material

1. Harper, S. Q. et al. Modular flexibility of dystrophin: implications for gene therapy of Duchenne muscular dystrophy. Nat Med 8, 253-61 (2002).
2. Scime, A. & Rudnicki, M. A. Molecular-targeted therapy for duchenne muscular dystrophy : progress and potential. Mol Diagn Ther 12, 99-108 (2008).
3. Fadel, P. J., Zhao, W. & Thomas, G. D. Impaired vasomodulation is associated with reduced neuronal nitric oxide synthase in skeletal muscle of ovariectomized rats. J Physiol 549, 243-53 (2003).
4. Duclos, F. et al. Progressive muscular dystrophy in alpha-sarcoglycan-deficient mice. J Cell Biol 142, 1461-71. (1998).
5. Grady, R. M. et al. Role for alpha-dystrobrevin in the pathogenesis of dystrophin-dependent muscular dystrophies. Nat Cell Biol 1, 215-20 (1999).
6. Pomplun, D., Mohlig, M., Spranger, J., Pfeiffer, A. F. & Ristow, M. Elevation of blood glucose following anaesthetic treatment in C57BL/6 mice. Horm Metab Res 36, 67-9 (2004).
7. Raisis, A. L. Skeletal muscle blood flow in anaesthetized horses. Part II: effects of anaesthetics and vasoactive agents. Vet Anaesth Analg 32, 331-7 (2005).
8. Voikar, V., Polus, A., Vasar, E. & Rauvala, H. Long-term individual housing in C57BL/6J and DBA/2 mice: assessment of behavioral consequences. Genes Brain Behav 4, 240-52 (2005).
9. Crosbie, R. H. et al. mdx muscle pathology is independent of nNOS perturbation. Hum Mol Genet 7, 823-9 (1998).
10. Durbeej, M. et al. Disruption of the beta-sarcoglycan gene reveals pathogenetic complexity of limb-girdle muscular dystrophy type 2E. Mol Cell 5, 141-51 (2000).
11. Lynch, G. S. et al. Contractile properties of diaphragm muscle segments from old mdx and old transgenic mdx mice. Am J Physiol 272, C2063-8 (1997).
12. Anderson, J. E. & Vargas, C. Correlated NOS-Imu and myf5 expression by satellite cells in mdx mouse muscle regeneration during NOS manipulation and deflazacort treatment. Neuromuscul Disord 13, 388-96 (2003).
13. Anderson, J. E., Weber, M. & Vargas, C. Deflazacort increases laminin expression and myogenic repair, and induces early persistent functional gain in mdx mouse muscular dystrophy. Cell Transplant 9, 551-64 (2000).
14. Archer, J. D., Vargas, C. C. & Anderson, J. E. Persistent and improved functional gain in mdx dystrophic mice after treatment with L-arginine and deflazacort. Faseb J 20, 738-40 (2006).
15. St-Pierre, S. J. et al. Glucocorticoid treatment alleviates dystrophic myofiber pathology by activation of the calcineurin/NF-AT pathway. Faseb J 18, 1937-9 (2004).
16. Hougee, S. et al. Oral administration of the NADPH-oxidase inhibitor apocynin partially restores diminished cartilage proteoglycan synthesis and reduces inflammation in mice. Eur J Pharmacol 531, 264-9 (2006).
17. Glowka, F. K. Stereoselective pharmacokinetics of ibuprofen and its lysinate from suppositories in rabbits. Int J Pharm 199, 159-66 (2000).
18. Gupta, M., Kovar, A. & Meibohm, B. The clinical pharmacokinetics of phosphodiesterase-5 inhibitors for erectile dysfunction. J Clin Pharmacol 45, 987-1003 (2005).

19. Takimoto, E. et al. Chronic inhibition of cyclic GMP phosphodiesterase 5A prevents and reverses cardiac hypertrophy. Nat Med 11, 214-22 (2005).
20. Walker, D. K. et al. Pharmacokinetics and metabolism of sildenafil in mouse, rat, rabbit, dog and man. Xenobiotica 29, 297-310 (1999).
21. Asai, A. et al. Primary role of functional ischemia, quantitative evidence for the two-hit mechanism, and phosphodiesterase-5 inhibitor therapy in mouse muscular dystrophy. PLoS ONE 2, e806 (2007).
22. Crosbie, R. H. et al. Membrane targeting and stabilization of sarcospan is mediated by the sarcoglycan subcomplex. J Cell Biol 145, 153-65 (1999).
23. Kameya, S. et al. alpha1-syntrophin gene disruption results in the absence of neuronal-type nitric-oxide synthase at the sarcolemma but does not induce muscle degeneration. J Biol Chem 274, 2193-200 (1999).
24. Eu, J. P. et al. Concerted regulation of skeletal muscle contractility by oxygen tension and endogenous nitric oxide. Proc Natl Acad Sci U S A 100, 15229-34 (2003).
25. Kinugawa, S. et al. Limited exercise capacity in heterozygous manganese superoxide dismutase gene-knockout mice: roles of superoxide anion and nitric oxide. Circulation 111, 1480-6 (2005).
26. Thomas, G. D. et al. Impaired metabolic modulation of alpha-adrenergic vasoconstriction in dystrophin-deficient skeletal muscle. Proc Natl Acad Sci U S A 95, 15090-5 (1998).
27. Wang, M. X. et al. Nitric oxide in skeletal muscle: inhibition of nitric oxide synthase inhibits walking speed in rats. Nitric Oxide 5, 219-32 (2001).
28. Seddon, M. D., Chowienczyk, P. J., Brett, S. E., Casadei, B. & Shah, A. M. Neuronal Nitric Oxide Synthase Regulates Basal Microvascular Tone in Humans In Vivo. Circulation, CIRCULATIONAHA.107.744540 (2008).
29. Perretti, M. & Ahluwalia, A. The microcirculation and inflammation: site of action for glucocorticoids. Microcirculation 7, 147-61 (2000).
30. Chao, D. S., Silvagno, F. & Bredt, D. S. Muscular dystrophy in mdx mice despite lack of neuronal nitric oxide synthase. J Neurochem 71, 784-9 (1998).
31. Wehling, M., Spencer, M. J. & Tidball, J. G. A nitric oxide synthase transgene ameliorates muscular dystrophy in mdx mice. J Cell Biol 155, 123-31 (2001).
32. Punkt, K. et al. Nitric oxide synthase is up-regulated in muscle fibers in muscular dystrophy. Biochem Biophys Res Commun 348, 259-64 (2006).
33. Cohn, R. D. et al. Prevention of cardiomyopathy in mouse models lacking the smooth muscle sarcoglycan-sarcospan complex. J Clin Invest 107, R1-7 (2001).
34. Tsunoda, M., Takezawa, K., Yanagisawa, T., Kato, M. & Imai, K. Determination of catecholamines and their 3-O-methyl metabolites in mouse plasma. Biomed Chromatogr 15, 41-4 (2001).
35. Barbato, J. C. Nicorandil: the drug that keeps on giving. Hypertension 46, 647-8 (2005).
36. Miki, T. et al. Mouse model of Prinzmetal angina by disruption of the inward rectifier Kir6.1. Nat Med 8, 466-72 (2002).
37. Stamler, J. S. & Meissner, G. Physiology of nitric oxide in skeletal muscle. Physiol Rev 81, 209-237 (2001).

38. Johnson, J. E., Wold, B. J. & Hauschka, S. D. Muscle creatine kinase sequence elements regulating skeletal and cardiac muscle expression in transgenic mice. Mol Cell Biol 9, 3393-9 (1989).
39. Sigmund, C. D. et al. Regulated tissue- and cell-specific expression of the human renin gene in transgenic mice. Circ Res 70, 1070-9 (1992).
40. Duclos, F. et al. Progressive muscular dystrophy in alpha-sarcoglycan-deficient mice. J Cell Biol 142, 1461-71 (1998).
41. Ervasti, J. M. & Campbell, K. P. Membrane organization of the dystrophin-glycoprotein complex. Cell 66, 1121-31 (1991).
42. Williamson, R. A. et al. Dystroglycan is essential for early embryonic development: disruption of Reichert's membrane in Dag1-null mice. Hum Mol Genet 6, 831-41 (1997).
43. Roberds, S. L., Anderson, R. D., Ibraghimov-Beskrovnaya, O. & Campbell, K. P. Primary structure and muscle-specific expression of the 50-kDa dystrophin-associated glycoprotein (adhalin). J Biol Chem 268, 23739-42. (1993).
44. Lebakken, C. S. et al. Sarcospan-deficient mice maintain normal muscle function. Mol Cell Biol 20, 1669-77. (2000).
45. Straub, V. et al. epsilon-sarcoglycan replaces alpha-sarcoglycan in smooth muscle to form a unique dystrophin-glycoprotein complex. J Biol Chem 274, 27989-96. (1999).